

See discussions, stats, and author profiles for this publication at: <https://www.researchgate.net/publication/263957484>

Optimum Solids Concentration in an Agitated Vessel

ARTICLE *in* INDUSTRIAL & ENGINEERING CHEMISTRY RESEARCH · FEBRUARY 2014

Impact Factor: 2.59 · DOI: 10.1021/ie402252c

CITATIONS

4

READS

70

4 AUTHORS, INCLUDING:



Rajarathinam Parthasarathy

RMIT University

111 PUBLICATIONS 323 CITATIONS

[SEE PROFILE](#)



Paul Slatter

RMIT University

91 PUBLICATIONS 570 CITATIONS

[SEE PROFILE](#)

Optimum Solids Concentration in an Agitated Vessel

Steven Wang,^{*,†} Rajarathinam Parthasarathy,^{*,§} Jie Wu,[‡] and Paul Slatter[§]

[†]Division of Earth Science and Resource Engineering, Commonwealth Scientific and Industrial Research Organization, Clayton, Victoria 3169, Australia

[‡]Division of Process Science and Engineering, Commonwealth Scientific and Industrial Research Organisation, Highett, Victoria 3190, Australia

[§]Rheology and Materials Processing Centre, School of Civil, Environmental and Chemical Engineering, RMIT University, Melbourne, Victoria 3001, Australia

ABSTRACT: Particle suspension in high-concentration slurries has been studied using radial-, mixed-, and axial-flow impellers. Impeller power measurements in this study were linked to the mass of solids suspended in the agitation system rather than the suspension volume. This approach was based on the consideration that the rate of dissolution or reaction depends to a large extent on the exposed surface area or mass of solids and might not be affected by the suspension volume, once off-bottom suspension is achieved. It was found that the specific power, based on the mass of solids, can be minimized by operating the system at relatively higher solids concentrations in the range of 0.20–0.35 (v/v) for the solids, impeller types, and geometrical conditions used in this work. Overall, improved energy efficiency can be achieved by using higher-power-number impellers under unbaffled conditions over a range of solids concentrations. A case example is illustrated to demonstrate the benefits of adopting some of the optimization methods highlighted in this article.

INTRODUCTION

Mechanically agitated vessels are widely used in industry for solid–liquid mixing in processing plants including for operations such as dispersion of solids, dissolution, crystallization, precipitation, adsorption, desorption, ion exchange, leaching, digestion, solid-catalyzed reaction, and suspension polymerization. Process intensification in these vessels often requires that the production yield per unit volume per unit time be increased without the need for major changes in the plant. Process intensification can be achieved by increasing the throughput or yield through improved physical processes such as efficient mixing because it is entirely impractical to reduce the size or volume of existing agitated tanks. In such instances, it is beneficial to maintain the vessel volume and intensify the process by increasing the solids throughput while minimizing the energy consumption. When the solids throughput is increased, the impeller speed required to suspend the solids off the tank bottom is increased, which consequently increases the energy input to the system. Therefore, it is essential to determine suitable mixing vessel and impeller configurations that can achieve the “just-suspended condition” for high-concentration slurries with minimum energy input.

One of the important operating parameters that determine the efficiency of solid–liquid mixing vessels is the critical impeller speed at which the just-suspended condition occurs, which is denoted as N_{js} . Energy input at N_{js} is regarded as a critical design factor for solid–liquid mixing vessels and it is a function of the process operating conditions, such as solids concentration, and geometric parameters, such as impeller and baffle types. Studies associated with solids suspensions in agitated vessels have been well documented over the past 40 years. Many researchers have investigated the effect of impeller diameter on N_{js} and concluded that N_{js} decreases with increasing impeller diameter for a given tank diameter.^{1–4}

Others have also evaluated the relationship between the impeller off-bottom clearance and N_{js} and found that reduction in N_{js} can be achieved by decreasing the off-bottom impeller clearance.^{1,5,6}

Reporting the impeller speed, rather than the power draw at complete suspension, has two drawbacks: (1) It is not possible to compare the energy efficiency or power consumption of a given system with other work, and (2) the estimates of the impeller power draw using N_{js} can be inaccurate by up to 20% because the power number at the complete suspension condition can be a function of solids concentration.^{7,8} Therefore, it is highly desirable to compare the efficiency of mixing systems in terms of the systems’ specific power input. Such a comparison can enable energy consumption reductions in inefficient processing plants such as mineral processing plants where a series of large and extremely energy-intensive solids suspension tanks are often used.

Researchers have focused on determining various ways to minimize energy consumption in slurry handling tanks. One of them is to implement different tank geometries. Kasat and Pandit⁹ concluded that the choice of a proper impeller for solid suspension is the key in achieving economic success in the process. Wu et al.¹⁰ found that the removal of baffles can play an effective role in dramatically reducing the power draw for suspending the particles off the tank bottom. They found that about a 70% energy saving can be achieved at high solids loading (>0.40) under unbaffled conditions. They also demonstrated that, under unbaffled conditions, axial impellers are more energy-intensive than radial impellers, which is

Received: July 15, 2013

Revised: January 31, 2014

Accepted: February 4, 2014

Published: February 4, 2014

contradictory to conventional findings.⁵ Despite these studies, there is a lack of understanding on impeller power consumption for solids suspension in agitated vessels, especially for those handling high-concentration slurries (>0.20 v/v). Most of the previous studies have used a limited range of solids concentrations (0.01–0.20 v/v).¹¹

Most of the previous work considered the impeller power input on the basis of the volume of the vessel or reactor.^{7,11} However, Dreher et al.¹² suggested that, except for processes, such as crystallization, that require suspension homogeneity, the rate of mass transfer or reaction is independent of agitation and the vessel volume once the suspension of solids is achieved. They suggested that, for such processes, the reaction rate is controlled by the solid surface area and, therefore, the volume of the reactor does not play a critical role. Based on that consideration, they used the specific power input expressed on the basis of the total mass of solids suspended to evaluate their experimental data. They reported that, when the specific power determined as the impeller power at the just-suspended condition (P_{js}) per unit mass of suspended solids (M_s) is plotted against the solid concentration, it has a minimum value at around 30% (v/v) solids. This finding was reported for all of the impeller types tested by the authors. This result is somewhat consistent with the results reported by Ragav Rao et al.,⁶ who found that P_{js}/M_s has a decreasing trend with increasing solids concentration. They found that less power input was required to suspend 6.6 wt % solids as compared to 0.34 wt % solids.

Expressing the impeller power draw at N_{js} on the basis of total solids mass, as was done by Dreher et al.,¹² is logical considering that, in many processes, such as leaching and digestion, the rate of reaction is largely influenced by the solid specific surface area. Therefore, it is appropriate to use a specific power expressed on the basis of the mass of suspended solids to determine the optimum solids concentration to be used in solid–liquid reactors. Since the attempt of Dreher et al.,¹² this approach to determine the optimum solids concentration has not been used in many studies and therefore warrants further investigation. Furthermore, Dreher et al.'s work focused mainly on solids suspension in baffled tanks. Considering that, as shown in refs 10 and 13, the removal of baffles leads to reductions in the impeller power draw for solids suspensions, it will be interesting to investigate the relationship between specific power in terms of the mass of solids and solids concentration in unbaffled tanks. In addition, it will be useful to investigate the effects of variables such as particle size, impeller type, and number of impellers on the specific power input based on total solid mass.

Zwietering⁵ introduced the visual observation method to determine N_{js} , which he defined as the impeller speed at which no solid particles can be observed to remain at rest on the tank bottom for more than 1 or 2 s. This criterion has frequently been used to measure N_{js} by many researchers.^{12,14} However, Kasat and Pandit⁹ pointed out that excess energy is required to lift small amounts of solids from relatively stagnant regions around the periphery of the vessel bottom, especially near baffles or at the center of the vessel bottom because liquid circulation is not strong enough there as compared to that in the bulk of the vessel. They also noted that, from a practical point of view, these regions are generally insignificant, but they could lead to a 20–50% increase in the impeller speed required for off-bottom suspension of solids. Wu et al.¹⁰ also pointed out that this definition is problematic in practice because a small

quantity of stationary particles in a corner might not be suspended even at a very high stirring speed and it is difficult to rely on the status of a small quantity of particles to determine the just-suspended condition. In addition, Zwietering's method is significantly influenced by subjective evaluation. Its repeatability is poor because of the complicated flow patterns in solid–liquid systems, particularly at high solids loadings [0.20–0.50 (v/v)].

In general, it should be noted that, for processes involving chemical reactions, the kinetics can be either diffusion-limited or non-diffusion-limited. For non-diffusion-limited processes, it is often sufficient to keep the solids just suspended off the tank bottom. Additional power input, which tends to increase suspension homogeneity, does not lead to increased reaction rates and, thus, is wasteful. Therefore, it is sufficient to consider the specific power input into the system at the just-off-bottom solids suspension condition. This is the basis on which all power measurements and analyses were carried out in this work.

This article describes a study investigating the impact of the solids loading on P_{js}/M_s in a 0.39-m agitated vessel. The results are applicable to the overall goal of developing optimized industrial agitators designed to minimize the power consumption for suspending a unit mass of solid particles in tanks, where the off-bottom solids suspension is a limiting factor.

■ EXPERIMENTAL SECTION

Experimental Equipment and Method. All experiments were carried out in a cylindrical, flat-bottomed perspex tank, with diameter $T = 0.39$ m, placed inside a rectangular outer glass tank (Figure 1). The cylindrical tank was equipped with four equally spaced baffles, each protruding a distance $B =$

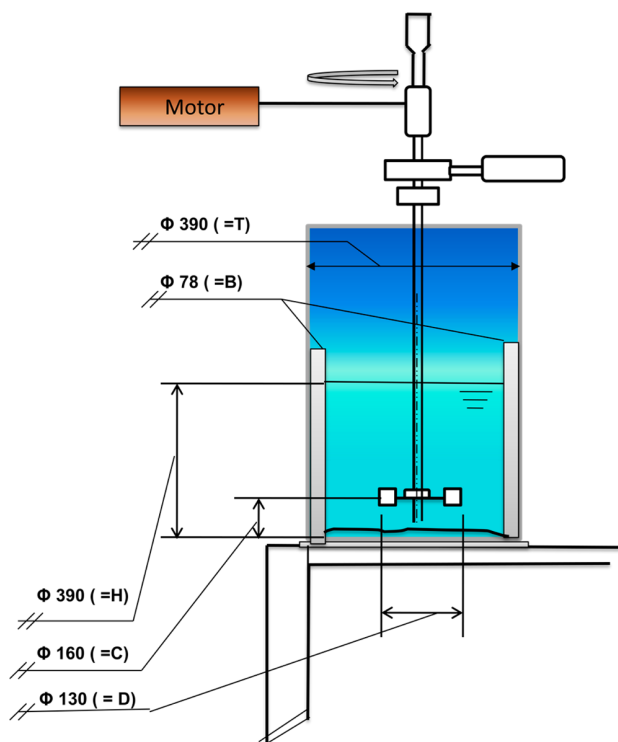


Figure 1. Schematic diagram of the experimental setup used in this study.

0.078 m into the tank, giving a width-to-tank diameter ratio (B/T) of 0.2. The space between the inner and outer tanks was filled with tap water, which helped to minimize the optical distortion caused by the curvature of the inner tank during flow visualization. The off-bottom impeller clearance was set to $T/3$. Impellers were mounted on a centrally driven shaft attached to an Ono Sokki torque transducer and a speed detector. The impeller shaft was driven by an electric motor having a maximum speed of 500 rpm. The shaft speed was varied using a variable-frequency drive.

Tap water was used as the liquid phase in all experiments. The liquid height in the inner tank (H) was maintained equal to the tank diameter. Spherical glass ballotini particles with a density of 2500 kg/m^3 were used as the solid particles. Three different types of glass particles (see Table 1) with mean particle sizes (d_{50}) of 90, 165, and $320 \mu\text{m}$ were used in this work.

Table 1. Particles Used in the Experiments

particle type	$d_{10} (\mu\text{m})$	$d_{50} (\mu\text{m})$	$d_{90} (\mu\text{m})$
A	70	90	100
B	110	165	235
C	260	320	480

The impellers used in this work are shown in Figure 2, and they consisted of a six-bladed Rushton turbine (DT6) with an impeller-diameter-to-tank-diameter ratio (D/T) of 0.4; two A310 impellers with D/T ratios of 0.4 and 0.5; and two 45° pitched-blade turbine impellers (45PBT4), both with a D/T

ratio of 0.4 but one with thicker blades (2 mm, $t/W = 0.125$) and the other with thinner blades (1 mm, $t/W = 0.062$). One mixed-flow impeller with six blades (30PBT6) was also used in this study. The other dimensions and details of the impellers are listed in Table 2. The impeller clearance from the tank

Table 2. Impeller Specifications and Power Number (N_p) Measured at the Nominal Impeller Clearance-to-Tank Diameter Ratio $C/T = 1/3$ and Impeller Diameter $D = 160 \text{ mm}$

impeller ID	full name	flow pattern	no. of blades	W/D^a	D/T^a	power no. (N_p)
DT6	Six-bladed radial disk turbine	radial	6	0.125	0.41	5.60
45PBT4	45° pitched four-bladed turbine	mixed	4	0.125	0.41	1.22
45PBT4	45° pitched four-bladed turbine	mixed	4	0.062	0.41	1.22
A310	Lightnin hydrofoil impeller	axial	3	0.125	0.46	0.32
A310	Lightnin hydrofoil impeller	axial	3	0.125	0.41	0.32
30PBT6	30° pitched six-bladed turbine	mixed	6	0.125	0.41	0.72

^a T , tank diameter; D , impeller diameter; W , blade width.

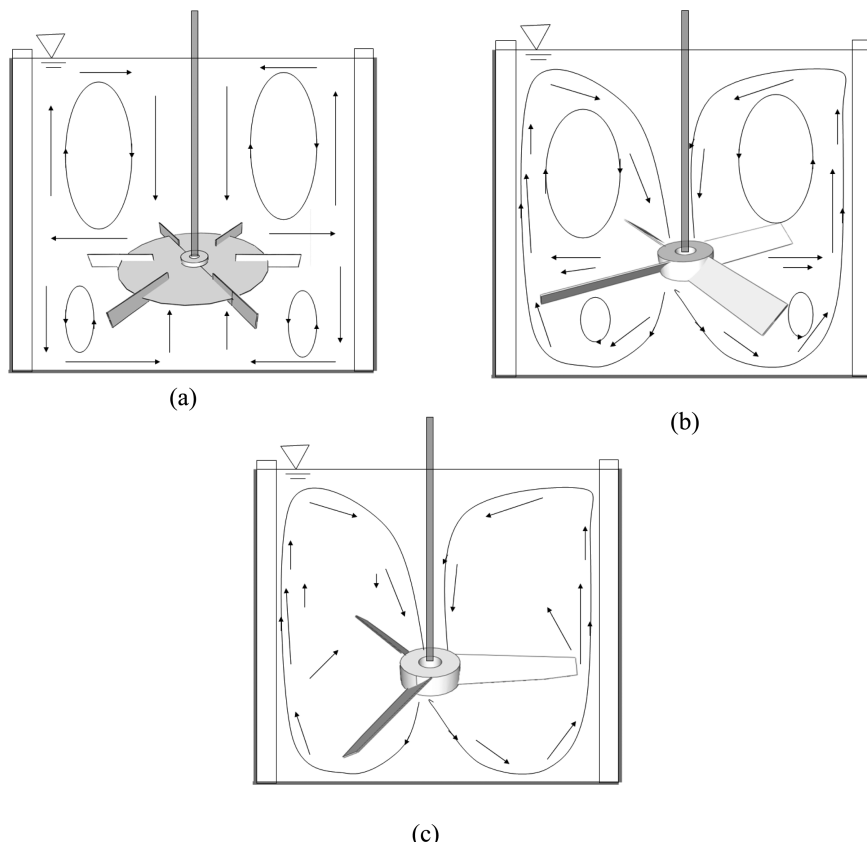


Figure 2. Impellers: (a) radial-flow impeller, DT6; (b) mixed-flow impeller, 45PBT4; (c) axial-flow impeller, A310.

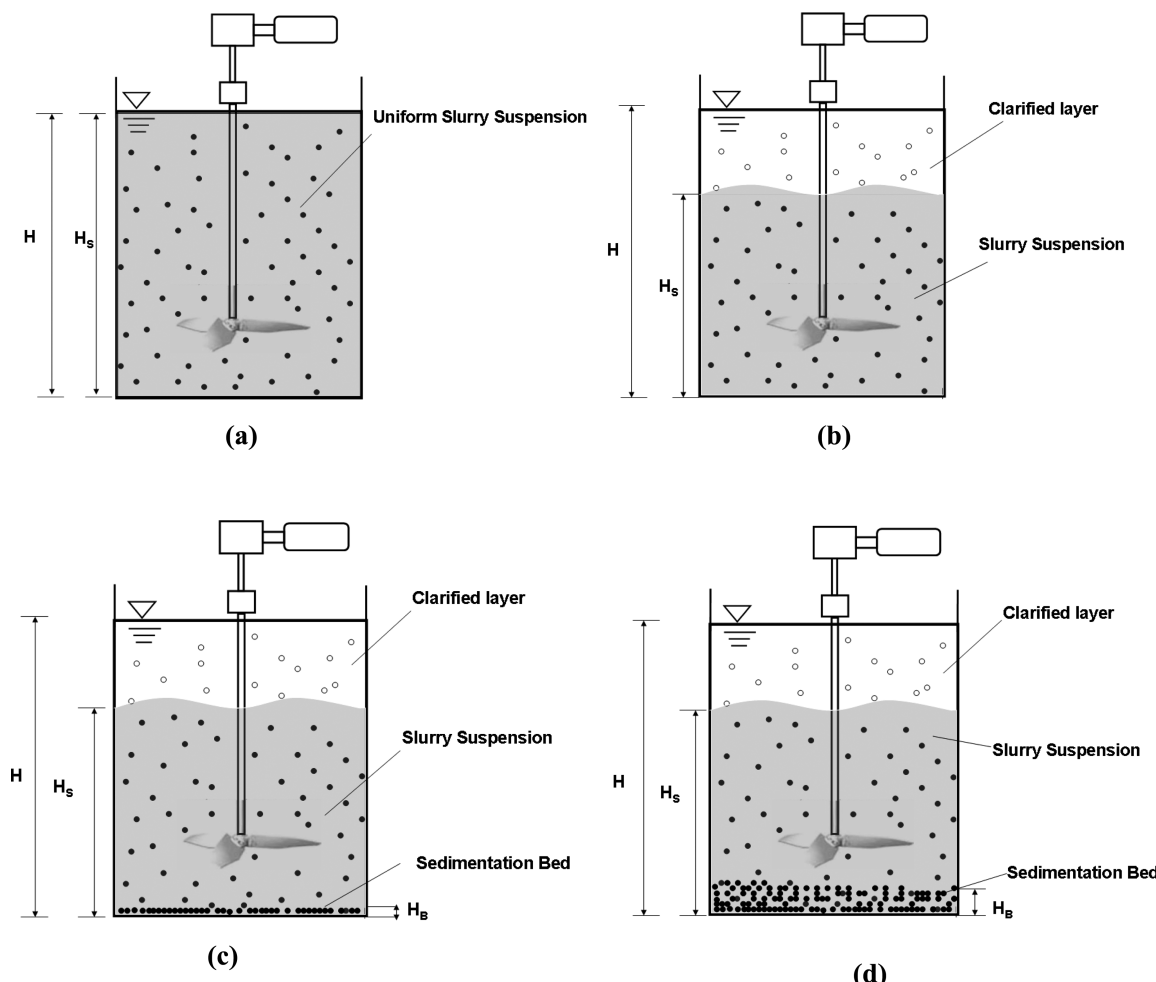


Figure 3. Visual method for determining N_{js} in solid–liquid mixing vessels: (a) $N > N_{js}$, homogeneous suspension, $H_s = H$; (b) $N = N_{js}$, $H_B = 0$; (c) $(N_{js} - N) \approx 2$ rpm, $H_B > 0$; (d) $N \ll N_{js}$, $H_B > 0$.

bottom was set at $T/3$, where T is the tank diameter. For the dual-impeller system, the impeller spacing was set equal to one impeller diameter (i.e., 160 mm).

Determination of the Critical Impeller Speed for the Just-Suspended Condition, N_{js} . In this work, a method proposed by Hicks et al.¹⁵ was used to determine N_{js} . In this method, the bed height of the solids settled at the tank bottom is used as a means of determining N_{js} . To determine N_{js} according to this method, the impeller speed is initially increased to a sufficiently high value so that no particles remain stationary at the tank bottom. At this condition, as shown in Figure 3a, all particles are moving freely within the liquid, and the suspension concentration is nearly uniform ($H_s \approx H$). The impeller speed is then decreased gradually until a thin layer of solid bed appears at the tank bottom (Figure 3b). The impeller speed is then increased slightly until the settled solid bed disappears. The speed at which the solid bed disappears is designated as N_{js} . If the impeller speed is decreased below N_{js} , a visible solid bed appears whose height is designated as H_B (Figure 3c,d). In this study, the height of the settled solid bed (H_B) was measured between two consecutive baffles. The ratio of the settled bed height (H_B) to the total liquid height (H) is plotted against the impeller speed in Figure 4 for impeller 30PBT6 to suspend solids at different concentrations. It can be seen that the normalized solid bed height is zero at N_{js} and it

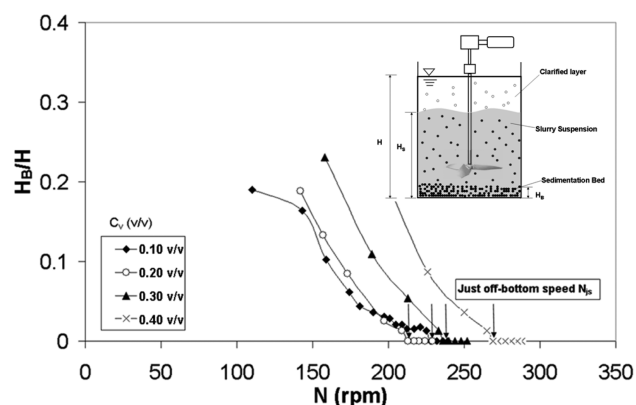


Figure 4. H_B/H vs N in a baffled tank, N_{js} determination at different solids concentrations. Impeller: 30PBT6.

increases with decreasing impeller speed. This method of using the settled solid bed height for determining N_{js} has been demonstrated to be quite reliable for suspensions with high solids concentrations.^{10,13}

Measurement of the Impeller Power Draw. The absolute torque, T_a , experienced by the impeller shaft was

measured using the torque transducer and determined according to the equation

$$T_a = T_m - T_r \quad (1)$$

where T_m is the torque measured during the experiments and T_r represents the residual torque due to mechanical friction in the bearing, which was determined by operating the impeller without the liquid and solid in the tank. The power consumption in the agitated system was then determined as

$$P = 2\pi NT_a = 2\pi N(T_m - T_r) \quad (2)$$

where P is the impeller power draw (W) and N is the impeller rotational speed in revolutions per second (rps). The specific power input, ϵ_{js} (W/kg), is defined as the impeller power draw, P (W), divided by the total solid mass in the suspension, M_s (kg), where

$$\epsilon_{js} = \frac{P_{js}}{M_s} = \frac{2\pi N_{js}(T_m - T_r)}{M_s} \quad (3)$$

It can be seen that the smaller the ϵ_{js} value, the less energy required to suspend the solids in the vessel.

RESULTS

Results are presented here to describe the effects of the solids concentration, impeller type, baffle, impeller dimensions, number of impellers, and particle size on the specific power input required to just suspend the particles. This leads to a discussion of the optimum solids concentration and the introduction of a simple model relating the power consumption to the solids concentration. Finally, an optimum agitator design is proposed based on the key findings of this study.

Effect of Solids Concentration. Values of the impeller power per unit slurry volume (P_{js}/V) required to just suspend the particles off the tank bottom are shown in Figure 5 as a

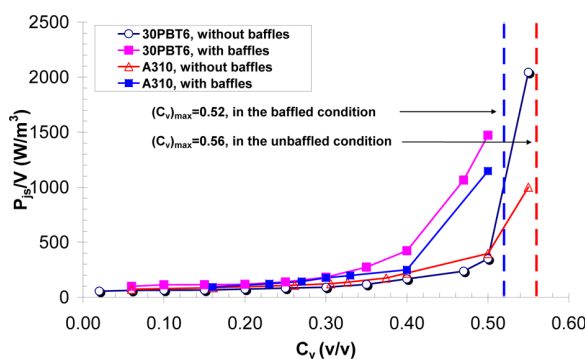


Figure 5. Variation of specific impeller power (P_{js}/V) with solids concentration. Solids: Glass particles of $d_{s0} = 0.165$ mm. Impellers: 30PBT6 and A310.¹⁶

function of solids concentration. The impellers used were a down-pumping 30° pitched-bladed turbine (30PBT6) and a hydrofoil impeller (A310). As expected, the specific power input (P_{js}/V) values for both A310 and 30PBT6 increased with increasing solids concentration in both baffled and unbaffled configurations. In each case, under baffled conditions, P_{js}/V increased gradually with increasing solids concentration up to 0.30 v/v and thereafter increased rapidly as the concentration approached the maximum achievable concentration of $(C_v)_{max} = 0.52$ v/v for this configuration.¹¹ Under baffled conditions,

regardless of the impeller type, the ratio of the maximum solids loading [$(C_v)_{max}$] to the solids packing coefficient (C_b) can be expressed as $(C_v)_{max}/C_b \approx 0.90$, where the value of the packing coefficient (C_b) was found to be 0.58 for the particles used in this study. Under unbaffled conditions, the maximum achievable solids concentration ($C_v)_{max}$ was found to be 0.56 v/v, which was higher than that under baffled conditions.¹⁶ Based on Figure 5, for the unbaffled tank, $(C_v)_{max}/C_b \approx 0.98$.

As shown in Figure 5, for all C_v values, P_{js}/V under unbaffled conditions was lower than that under baffled conditions.¹⁶ These results show clearly that the removal of baffles is highly beneficial in decreasing the impeller power input, especially when very high solids concentrations are used. Among the many possible reasons for the increased P_{js}/V values at high C_v , increased slurry viscosity could be the main one. Values of the slurry viscosity predicted using different correlations, reported by Honek et al.,¹⁷ are shown in Figure 6 for a range of C_v

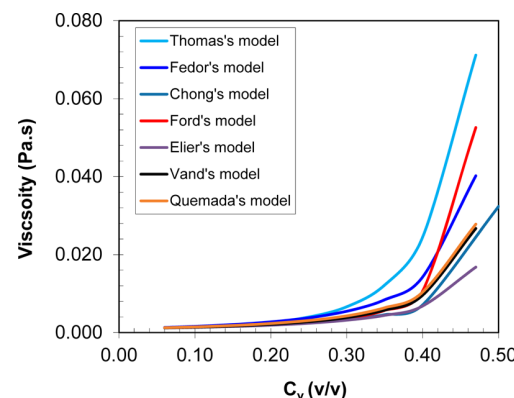


Figure 6. Effect of solids concentration on viscosity (viscosity calculations based on correlations reported by Honek et al.¹⁷).

values. These correlations are based on C_b and C_v . The influence of the solids loading on the slurry viscosity was not found to be significant in the range $0.15 < C_v < 0.40$ v/v. However, as C_v increased beyond 0.40 v/v, the effective viscosity increased steeply. This increase could possibly cause a sudden change in the fluid flow pattern, most likely from turbulent to transitional or even laminar flow. At such high solids concentrations, turbulence is most likely to be suppressed as a result of the solids packing effect. Therefore, it is not surprising to see a sharp rise in impeller specific power draw at ultrahigh solids concentrations.

As mentioned above, another measure by which the power input at N_{js} can be expressed is on the basis of the mass of solids suspended. The power input per unit mass of solids, ϵ_{js} , is defined in eq 3. Experimental data for ϵ_{js} at N_{js} are shown in Figure 7a as a function of C_v for impeller 30PBT6 under baffled conditions. It is interesting to note that, contrary to expectations, the ϵ_{js} value did not increase with increasing C_v . Instead, ϵ_{js} decreased with increasing C_v until a critical value was reached, and thereafter, it began to increase again. This trend was observed with ϵ_{js} values for other impellers as well.¹⁶

The C_v value at which ϵ_{js} is a minimum can be designated as the optimum solids concentration, $(C_v)_{osc}$, because it represents conditions at which the energy input into the system through impeller rotation is applied most efficiently. The $(C_v)_{osc}$ value for impeller 30PBT6 was found to be 0.25 v/v, as can be seen in Figure 7a. It is interesting to note that ϵ_{js} at 0.06 v/v was 3

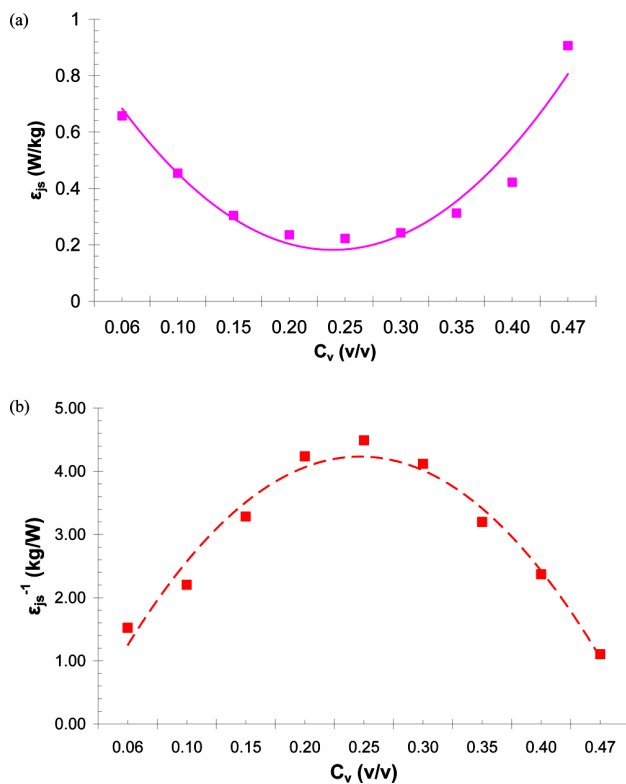


Figure 7. Variations of (a) specific power ($\epsilon_{js} = P_{js}/M_s$) and (b) ϵ_{js}^{-1} values with solids concentration when baffled. Impeller: 30PBT6. Solids: Glass particles of $d = 0.165$ mm.

times greater than that at $(C_v)_{osc} = 0.25$ v/v. Similar trends were observed for other impellers under unbaffled conditions as well. These results suggest that operating the process around $(C_v)_{osc}$ is better than operating at lower C_v values because slurries with higher solids concentrations can be suspended with a lower specific power input.

The increased impeller energy efficiency that can be obtained for solids suspension at higher C_v values can be demonstrated better by using the inverse of ϵ_{js} , as given by

$$\epsilon_{js}^{-1} = \frac{M_s}{P_{js}} \quad (4)$$

The ϵ_{js} data shown in Figure 7a for impeller 30PBT6 were used to plot Figure 7b, which shows ϵ_{js}^{-1} versus C_v . The parameter ϵ_{js}^{-1} represents the amount of solids that can be suspended per unit of impeller power input at N_{js} , and its units are kilograms of solids suspended per Watt. With increasing C_v , the ϵ_{js}^{-1} value increases, reaches a maximum at $(C_v)_{osc}$, and then decreases beyond that. It is interesting to note that, for each Watt of power input, about 4.5 kg of solids can be suspended at $(C_v)_{osc} = 0.25$ v/v whereas only 1.9 kg of solids can be suspended at $C_v = 0.05$ v/v. These results indicate that the impeller energy efficiency in solid–liquid mixing vessels can be increased by operating them at higher solids concentrations [around $(C_v)_{osc}$] than hitherto thought. It is also clear that operating the process at a lower solids concentration is not preferable because most of the impeller power input is utilized in pumping and moving the liquid without a proportional increase in solid suspension benefits, thereby leading to inadequate usage of the tank infrastructure.

The value of $(C_v)_{osc}$ is most likely determined by changes in the slurry flow pattern in the tank at this solid concentration. Changes in the slurry flow pattern can be identified from the impeller Reynolds number, which can be defined for a solid–liquid agitated tank as

$$Re = \frac{\rho_{slurry} N_{js} D^2}{\eta_{slurry}} \quad (5)$$

where ρ_{slurry} is the slurry density (kg/m^3), N_{js} is the just-off-bottom-suspension impeller speed (rps), D is the impeller diameter, and η_{slurry} is the slurry viscosity ($\text{Pa}\cdot\text{s}$) at N_{js} . The precise calculation of an average Reynolds number in a solid–liquid mixing system is complex due to the fact that the homogeneity of the suspension varies with location and there is an axial/radial solids concentration gradient. In this instance, it was assumed that the particles were evenly distributed throughout the tank for the sake of calculating a characteristic Reynolds number. The slurry viscosity, η_{slurry} , was calculated using the equations

$$\eta_{slurry} = \eta_r [1 + 2.5C_v + 10.05C_v^2 + 0.0273 \exp(16.6C_v)] \quad (6)$$

$$\eta_{slurry} = \eta_r \left(1 + \frac{1.25C_v}{C_b - C_v}\right)^2 \quad (7)$$

as suggested by Thomas¹⁸ and Fedors,¹⁹ respectively. In these equations, η_r is the viscosity of the carrier liquid, and C_b is the solids packing coefficient. The impact of the solids loading on Re for impeller 30PBT6 under baffled and unbaffled conditions is shown in Figure 8a,b. It can be seen that Re decreased with increasing C_v , regardless of the baffle arrangement. From Figure 8b, it is also clear that, at $C_v \geq (C_v)_{osc}$, the Re value decreased below 10000, indicating that the flow regime in the tank could have been changing from the turbulent to the transition flow regime as C_v increased. It should be noted that eqs 6 and 7 assume that the particles are uniformly distributed throughout the tank whereas, in reality, this is not often the case. Consequently, the Reynolds numbers in Figure 8a,b are approximate values. This probably explains why, in Figure 8a, Re at $(C_v)_{osc}$ is not around 10000. On the other hand, as C_v approaches the maximum achievable solids concentration, $(C_v)_{max}$, the flow regime will change to laminar. Under this condition, the turbulence that is responsible for solids suspension will be damped significantly, thereby leading to an excessive impeller power draw for achieving just-off-bottom suspension.

Effect of Impeller Type. Values of the specific impeller power input ϵ_{js} as a function of solids concentration for impellers DT6, 45PBT4, and A310 under baffled conditions are shown in Figure 9a.¹⁶ The impellers were chosen to represent the three flow types, namely, radial, mixed, and axial flow, respectively. The results shown in this figure confirm that an optimum solids concentration, $(C_v)_{osc}$, exists for all three types of impellers. The $(C_v)_{osc}$ value for impeller DT6 is around 0.35 v/v, whereas it is around 0.30 v/v for impellers 45PBT4 and A310. The corresponding ϵ_{js} values at $(C_v)_{osc}$ for impellers DT6, 45PBT4, and A310 are 0.79, 0.23, and 0.21 W/kg, respectively (with ϵ_{js}^{-1} values of 1.27, 4.35, and 4.79 kg/W, respectively). It can be also seen that the effect of the solids concentration on ϵ_{js} is more pronounced for impeller DT6, as demonstrated by the U-shaped curve for this impeller. For all

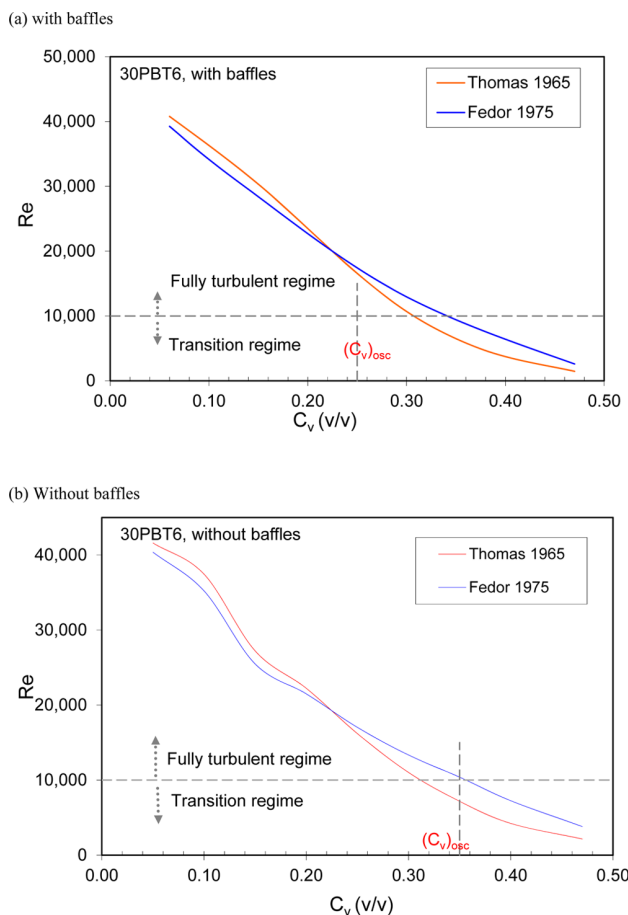


Figure 8. Effect of solids concentration on Reynolds number (Re) at N_{js} : (a) 30PBT6, baffled; (b) 30PBT6, unbaffled. (Viscosity calculations based on correlations reported by Honek et al.¹⁷)

solids concentrations (0.05–0.4 v/v), the ϵ_{js} values were found to be the highest for impeller DT6, followed by impeller 45PBT4. Impeller A310 had the lowest ϵ_{js} values. The relatively flat curve observed for impeller A310 suggests that the effect of the solids concentration on ϵ_{js} is not as significant for this impeller compared to the other two.

The ϵ_{js} data for the same impellers under unbaffled conditions are shown in Figure 9b.¹⁶ In this case also, the ϵ_{js} versus C_v curves have a minimum corresponding to $(C_v)_{osc}$. It is interesting to see that, under unbaffled conditions, impeller DT6, which had the highest power number ($N_p = 5.6$), was more energy efficient than impellers 45PBT4 ($N_p = 1.22$) and A310 ($N_p = 0.32$), irrespective of the value of C_v . For a given C_v , impeller DT6 had the lowest ϵ_{js} value over the whole range of C_v values used in this work (Figure 9b). Whereas the difference in the ϵ_{js} values of the three impellers was obvious at low C_v (<0.20 v/v), it became marginal as C_v approached 0.4 v/v. At $C_v = 0.40$ v/v, the three impellers had approximately the same ϵ_{js} values.

It has been well established that it is more energy efficient to employ impellers with lower power numbers, for example, axial-flow impellers, for off-bottom solids suspension. The results shown in Figure 9a indicate that this is indeed true under baffled conditions. However, under unbaffled conditions, the radial-flow impeller (DT6) was found to become more energy efficient compared to the mixed-flow (30PBT6) and axial-flow

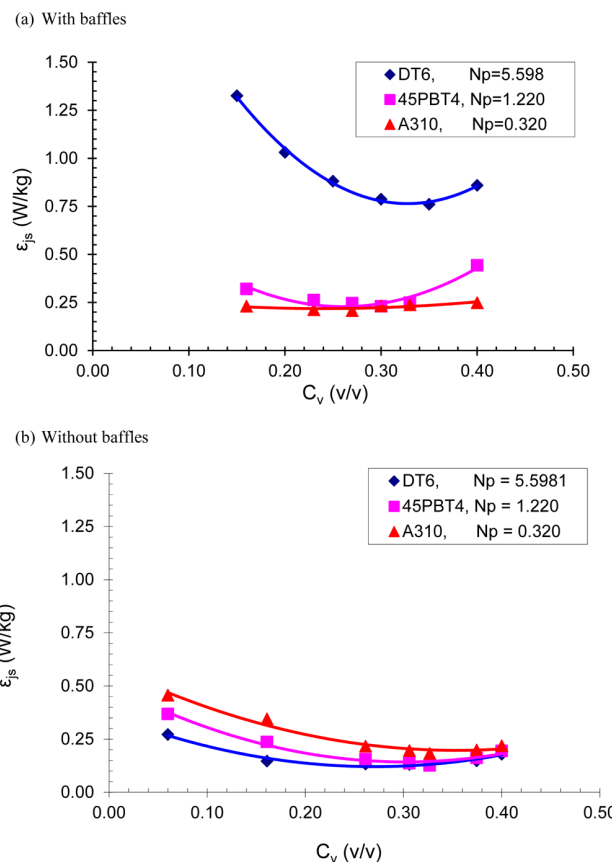


Figure 9. Effects of impeller type on ϵ_{js} when (a) baffled and (b) unbaffled.¹⁶ Glass particles of $d_{50} = 0.165$ mm. Impellers: DT6, 45PBT4, and A310.

(A310) impellers. These results indicate that radial-flow impellers with higher power numbers could be more energy efficient in suspending particles off the tank bottom. This trend was found to be true even for particles with different sizes, as shown later in this article.

Effect of Baffle Removal on ϵ_{js} Reduction. The ϵ_{js} values for impellers DT6, 45PBT4, and A310 under baffled and unbaffled conditions are shown in Figure 10 in the form of a bar graph for a few chosen C_v values. The extent of the reduction in ϵ_{js} due to the removal of baffles can be seen clearly from this graph. It is also clear that the reduction in ϵ_{js} is influenced by both the impeller type and the solids concentration. The reduction in ϵ_{js} was most pronounced for impeller DT6. A significant ϵ_{js} reduction of up to 90% was achieved for this impeller over the C_v range of 0.16–0.4 v/v simply by removing the baffles (Figure 10a). Reductions in ϵ_{js} due to the removal of baffles were also observed for impellers 45PBT4 and A310, but the extents of the reductions were lower compared to that for DT6. For impeller 45PBT4, the extent of ϵ_{js} reduction was higher at higher C_v values, contrary to what was observed for impeller DT6 (Figure 10b). For impeller A310, there was no clear trend in the extent of ϵ_{js} reduction as a function of C_v (Figure 10c). Based on these results, it can be concluded that the extent of ϵ_{js} reduction due to the removal of baffles is more significant for radial-flow impellers, followed by mixed-flow impellers. The impact for axial-flow impellers seems to be relatively insignificant.

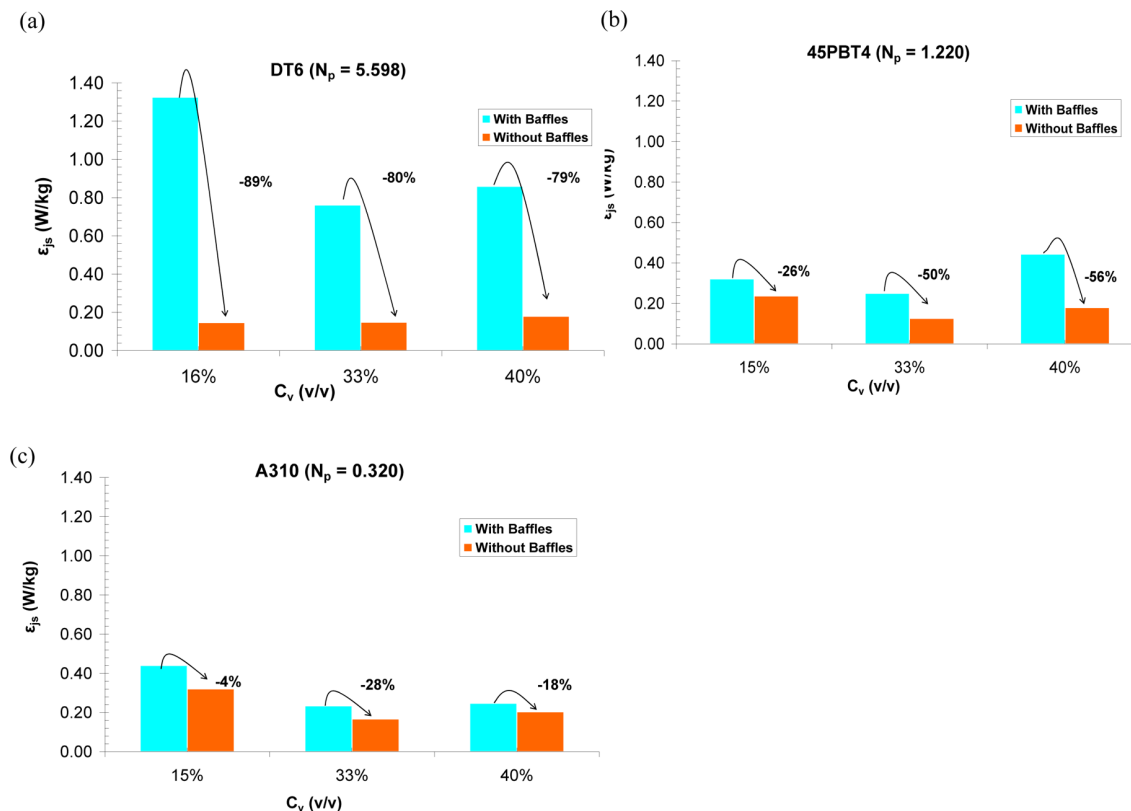


Figure 10. Effect of baffle removal on ϵ_{js} reductions for impellers (a) DT6 ($N_p = 5.60$), (b) 45PBT4 ($N_p = 1.22$), and (c) A310 ($N_p = 0.32$). Solids: Glass particles of $d_{50} = 0.165$ mm.

To analyze the reduction in impeller power consumption due to the removal of baffles, the impeller power number N_p at N_{js} was calculated according to the equation

$$N_p = \frac{P_{js}}{\rho_{\text{slurry}} N_{js}^3 D^5} \quad (8)$$

where ρ_{slurry} is the slurry density (kg/m^3), P_{js} is the impeller power at N_{js} (W), N_{js} is the just-off-bottom-suspension impeller speed (rps), and D is the impeller diameter (m). N_p at N_{js} values for impellers DT6, 45PBT4, and A310 are shown in panels a–c, respectively, of Figure 11 as a function of C_v . The N_p at N_{js} values under unbaffled conditions were found to be lower than those under baffled conditions regardless of the C_v value and impeller type. These results also indicate that the extent of reduction in N_p was most pronounced for impeller DT6, followed by impeller 45PBT4 and then impeller A310.

The significant increase in impeller power reduction observed for impeller DT6 due to the removal of baffles can be attributed to the reduction in energy dissipation on the vessel walls when the baffles were removed. In a fully baffled vessel, the liquid jet stream generated by the impeller rotation impinges directly on the tank wall, leading to a reduction in its energy. In contrast, in an unbaffled tank, the liquid pumped by the impeller follows a tangential motion, which causes it to circulate with minimum deflections off the tank wall, thereby leading to a reduction in drag loss and energy dissipation. Dreher et al.⁷ suggested that the absence of baffles in the lower part of the tank leads to an inward-spiralling flow pattern at the vessel base that sweeps any settled solids toward the center of the base from where they are suspended due to the suction of a

vortex formed under the impeller. In addition to the vortex under the impeller, solids suspension is probably also helped by the secondary circulation loop above the impeller, especially for impeller DT6. This suggestion is based on the observation in this work that the slurry height (H_s) at N_{js} was always higher for impeller DT6 than that for the axial-flow impeller used in this work. Geisler et al.²⁰ suggested that solids suspension in stirred vessels is dependent on particle pick-up off the tank bottom and continuous circulation of fresh liquid from the supernatant into the suspended slurry, which ensures particle suspension in the upper parts of the tank. This mechanism is very helpful in the suspension of slurries at higher solids concentrations. It can be anticipated that the flow circulation loop generated by a Rushton turbine contributes significantly to the entrainment of the supernatant in the upper region of the vessel, leading to higher degree of suspension (i.e., high H_s) and improved energy efficiency (i.e., low ϵ_{js}).

Effect of Impeller Dimensions (D/T , t/W). The effect of the impeller diameter on ϵ_{js} is shown in panels a and b of Figure 12 for baffled and unbaffled tanks, respectively. Experiments were conducted for a solids concentration range of 0.10–0.40 v/v. Two A310 impellers of 0.16- and 0.20-m diameter, pumping downward, were employed in the tests. Under unbaffled conditions, the effect of impeller diameter was marginal on ϵ_{js} at high solids concentrations ($C_v > 0.30$ v/v). This is consistent with the results reported by others.^{10,13} However, this finding has to be verified for other impeller types as well. From Figure 12b, it is evident that, under unbaffled conditions, an increase in impeller diameter led to a decrease in ϵ_{js} (~0.2 W/kg) over the whole range of C_v values used in this work. The parallel curves for ϵ_{js} indicate that the ratio of ϵ_{js}

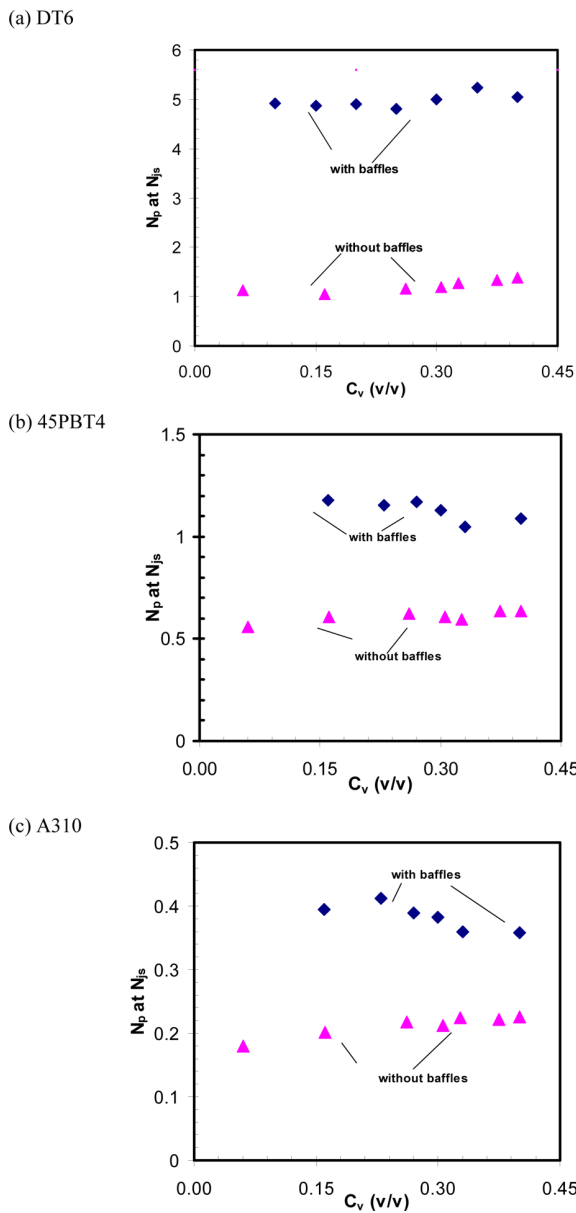


Figure 11. Effect of baffle removal on power number for impellers (a) DT6, (b) 45PBT4, and (c) A310. Solids: Glass particles of $d_{50} = 0.165$ mm.

values for the two impellers with different diameters was fairly constant under unbaffled conditions.

The effect of blade thickness on ϵ_{js} is shown for impeller 45PBT4 in Figure 13. It can be seen that the variation of ϵ_{js} with C_v depends on blade thickness. At the minimum value of ϵ_{js} , $(C_v)_{osc}$ was 0.25 v/v for the impeller with the thinner blade ($t/W = 0.062$) but 0.30 v/v for the impeller with the thicker blade ($t/W = 0.125$). However, the ϵ_{js} values at $(C_v)_{osc}$ for both impellers were nearly the same. It is also clear that the ϵ_{js} value for the impeller with the thinner blade ($t/W = 0.062$) was lower for $C_v < 0.27$ v/v, suggesting that this impeller is more efficient in this range. For $C_v > 0.27$ v/v, the impeller with the thicker blade had a lower ϵ_{js} value, indicating that it is preferable to use the impeller with a thicker blade for high C_v .

In general, it can be concluded that D/T does not have a significant impact on the value of the optimum solids

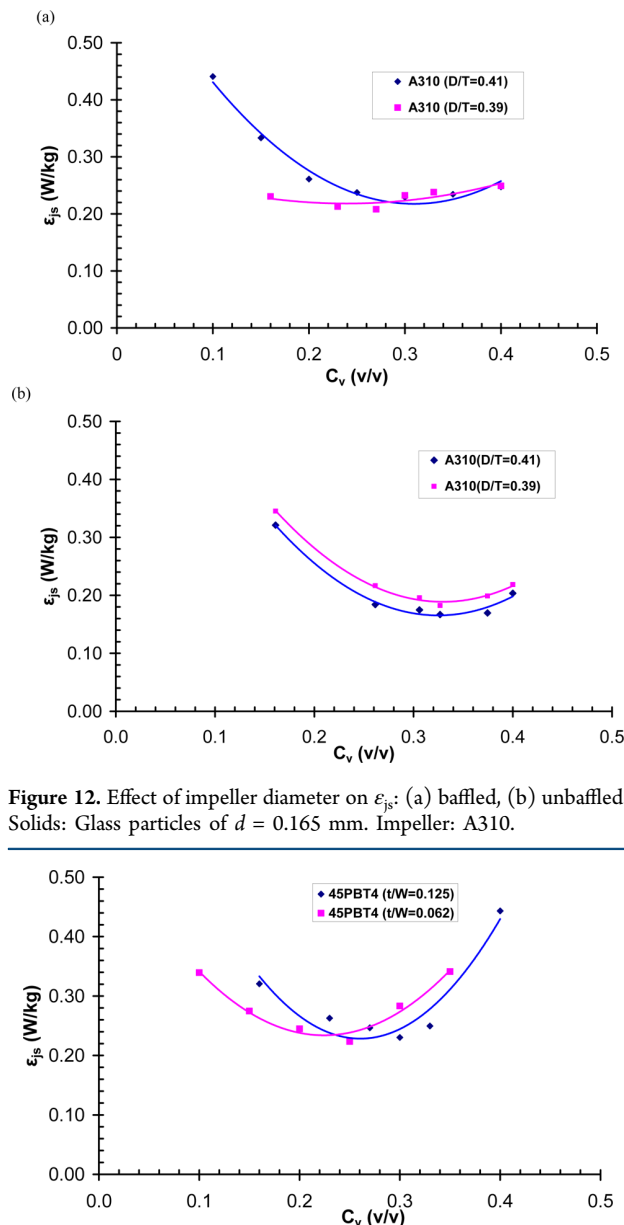


Figure 12. Effect of impeller diameter on ϵ_{js} : (a) baffled, (b) unbaffled. Solids: Glass particles of $d = 0.165$ mm. Impeller: A310.

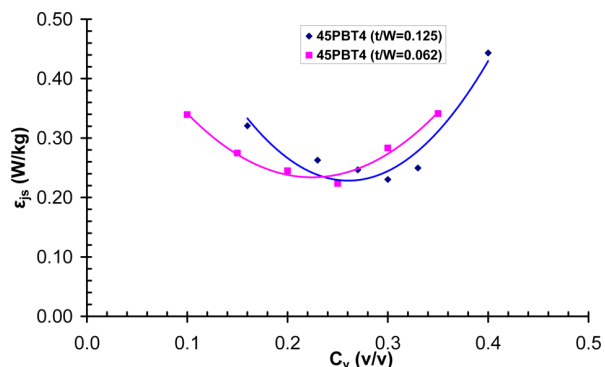


Figure 13. Effect of blade thickness on ϵ_{js} when baffled. Solids: Glass particles of $d = 0.165$ mm. Impeller: 45PBT4. (t = impeller thickness, W = impeller width.)

concentration in a mixing tank. However, a slight change in t/W leads to a shift in $(C_v)_{osc}$, and a larger t/W value leads to a greater value of $(C_v)_{osc}$.

Effect of Multiple Impellers. The ϵ_{js} data for a dual A310 impeller and a single A310 impeller, both with $D/T = 0.41$, are shown in Figure 14 as a function of C_v under unbaffled conditions. It is interesting to note that the $(C_v)_{osc}$ value for the dual A310 system is similar to that of the single A310 impeller. At low C_v (<0.3 v/v), the presence of the additional impeller led to a higher ϵ_{js} value because of the interaction of the flow patterns generated by the two impellers.^{21–23} It can be also said that the increase in ϵ_{js} with an additional impeller was marginal (<3%) at high C_v . This finding has not been verified for other impeller types or baffled conditions.

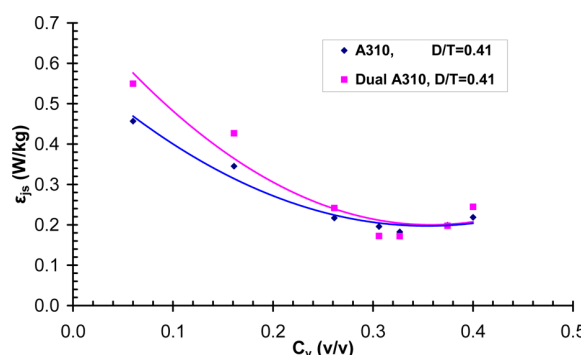


Figure 14. Effect of dual impellers on ϵ_{js} when baffled. Solids: Glass particles of $d = 0.165 \text{ mm}$. Impeller: A310.

It is reasonable that a dual impeller would have higher ϵ_{js} values at low C_v . In such cases, the lower impeller is responsible for solids suspension, as reported by Armenante and Li,²¹ and the upper impeller does not contribute much to the just-off-bottom condition but does contribute to additional impeller power draw, thereby leading to higher ϵ_{js} values. At high C_v , the upper impeller would also contribute to solids suspension because of the enhanced pumping in the upper region of the tank, which would ensure an even distribution of solid particles and, therefore, lower ϵ_{js} values.

Effect of Particle Size. The influence of particle size on ϵ_{js} under unbaffled conditions is shown in Figure 15 for the three impellers used in this work. The three mean particle sizes used

in this study were 90, 165, and 320 μm . It can be seen that coarser particles led to higher ϵ_{js} values, irrespective of the impeller type and solids concentration. These results indicate that it is more energy efficient to suspend a large number of small particles than a small number of large particles for the same amount of solids mass. This is a useful observation with a number of practical implications. For example, in the mineral processing industry, it is well-known that the energy required to grind ore into fine particles is very high. However, when considering the overall energy usage, there is a benefit in handling slurries with fine particles because the reduction in ϵ_{js} for suspending fine particles in agitated vessels could partially compensate for the higher energy usage expended in grinding ore into fine particles, thereby leading to overall energy efficiency in the process.

Drewer et al.¹² evaluated the effect of particle size on the specific power in a baffled tank and reported that $(C_v)_{osc}$ is not affected by particle size but is influenced by impeller type (Figure 16a). They also found that an increase in particle size resulted in higher power consumption at the just-suspended condition. The effects of particle size on $(C_v)_{osc}$ and the corresponding ϵ_{js} value observed in this work are shown in Figure 16b. These results also imply that $(C_v)_{osc}$ is not affected by the impeller type for a given particle diameter d_p under unbaffled conditions. In contrast, $(C_v)_{osc}$ was found to decrease with increasing d_p , irrespective of the impeller type. Also, ϵ_{js} was found to increase dramatically with increasing d_p . However, more experiments with a wide range of d_p values are required to

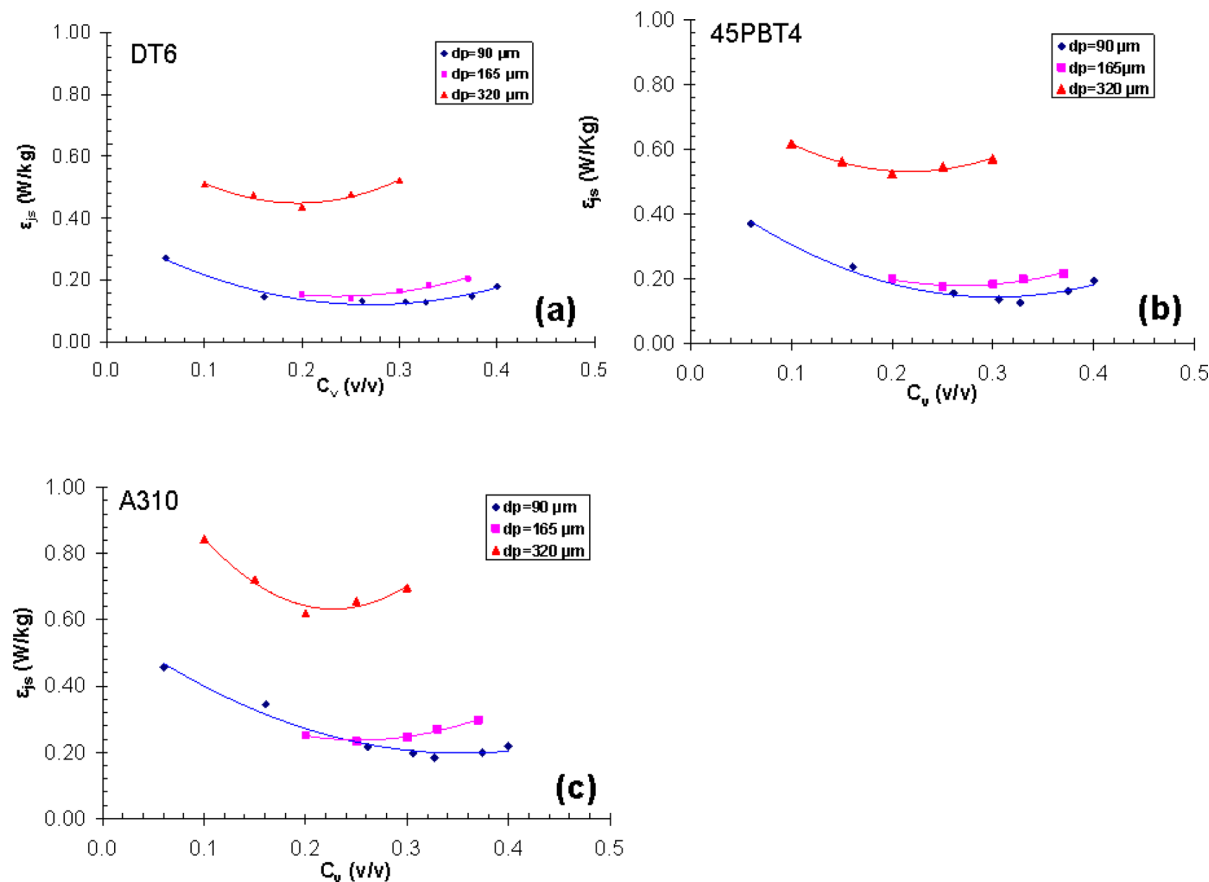


Figure 15. Effect of particle size on ϵ_{js} when baffled. Impeller: (a) DT6, (b) 45PBT4, and (c) A310. Solids: Glass particles.

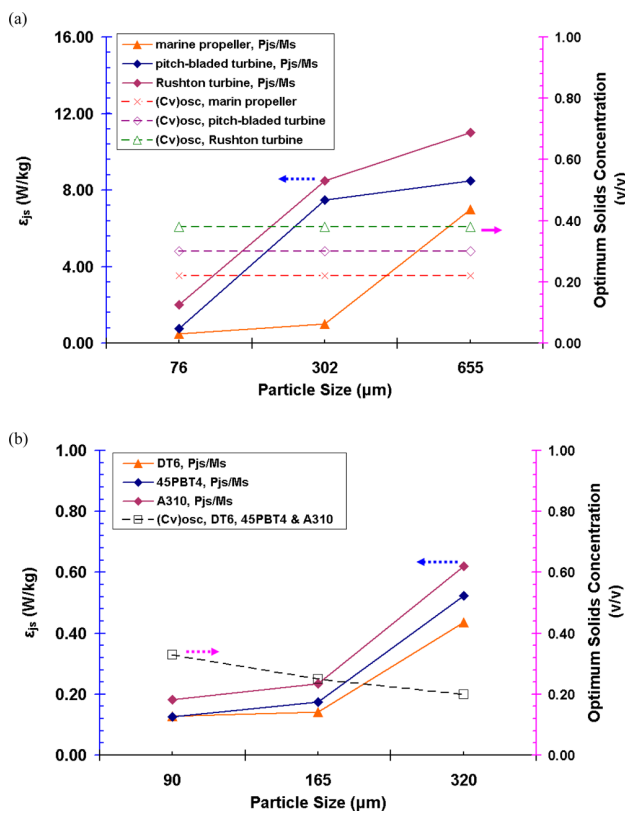


Figure 16. Effect of particle size on optimum solids concentration (C_v)_{osc} and corresponding ϵ_{js} value: (a) baffled,¹² (b) unbaffled.

confirm the relationship between ϵ_{js} and C_v under baffled conditions.

Optimum Solids Concentration. The specific power required for the complete suspension of solids for a range of solids concentrations and particle sizes was discussed above. It was confirmed that ϵ_{js} can be minimized by operating agitated vessels at an optimum solids concentration, (C_v)_{osc}. Tables 3 and 4 summarize the (C_v)_{osc} and corresponding (ϵ_{js})_{min} values for different impellers and particle sizes under baffled and unbaffled conditions, respectively.

Table 3. Optimum Solids Concentrations and Corresponding (ϵ_{js})_{min} Values under Baffled Conditions^a

impeller specifications				
	D/T	W/D (%)	(C_v) _{osc} (% v/v)	(ϵ_{js}) _{min} (W/kg)
DT6	0.41	9.4	35	0.76
A310	0.46		30	0.23
A310	0.41		27	0.21
45PBT4	0.41	4.7	30	0.23
45PBT4	0.41	9.4	25	0.22
30PBT6	0.41	9.4	25	0.22

^a $d_p = 120 \mu\text{m}$.

Under baffled conditions, (C_v)_{osc} is influenced by the impeller type and dimensions. However, (C_v)_{osc} = 0.30 v/v is a representative value that can be used for all impellers used in this work. Under unbaffled conditions, it can be concluded that (C_v)_{osc} is independent of impeller type but influenced by d_p . It was found that an increase in d_p leads to a decrease in (C_v)_{osc}.

Table 4. Optimum Solids Concentrations and Corresponding (ϵ_{js})_{min} Values under Unbaffled Conditions^a

impeller specifications	D/T	W/D (%)	d_p (μm)	(C_v) _{osc} (v/v)	(ϵ_{js}) _{min} (W/kg)
DT6	0.41	9.4	120	33	0.13
DT6	0.41	9.4	165	25	0.14
DT6	0.41	9.4	320	20	0.44
A310	0.41		120	33	0.18
A310	0.46		120	33	0.17
dual A310	0.41		120	33	0.17
A310	0.41		165	25	0.23
A310	0.41		320	20	0.62
45PBT4	0.41	9.4	120	33	0.12
45PBT4	0.41	9.4	165	25	0.17
45PBT4	0.41	9.4	320	20	0.52

^aImpeller clearance-to-tank diameter ratio: $C/T = 1/3$.

The presence of a minimum ϵ_{js} value in ϵ_{js} versus C_v graphs suggests that there are some advantages in operating mixing tanks at higher C_v values than are generally used now. In the design of a new plant, an increase in C_v would result in the reduction of vessel and impeller sizes for a given mass throughput. As a consequence, capital costs can be reduced significantly. Also, the (C_v)_{osc} value corresponding to the minimum ϵ_{js} value has practical implications for the operation of slurry suspension vessels. Any solid–liquid mixing vessel designed based on the above criteria will lead to lower operating costs with optimum energy/power efficiency. Operating solid–liquid mixing tanks with a dilute or relatively low C_v value is certainly not beneficial to industry from a practical point of view, because operating costs will be unnecessarily higher due to insufficient usage of existing infrastructure. Also, low solids concentrations are not beneficial to mixing intensification, which is a means to significantly increase the yield per unit volume per unit time.

The benefits of operating a solid–liquid mixing process at the (C_v)_{osc} are yet to be fully exploited in industry. Wang et al.¹⁶ considered various ways of improving the energy efficiency in a solid–liquid mixing tank by optimizing impeller design and tank geometry. It has been shown that significant gains in energy efficiency can be achieved by removing baffles, which are conventionally installed in most slurry tanks. However, a side effect of removing the baffles is increased mixing times.¹³ This is usually not a problem in the mining/mineral processing industry, where the time scales for reactions or mass transfer in slurry tanks are typically an order of magnitude greater than the mixing time. In some cases, even mixing is not required. An example is slurry holding tanks, where the slurry is held to smooth out fluctuations in the slurry flow rate that occur as a result of variations in the throughput in other equipment in the continuous process circuit. In addition to the removal of baffles, it is possible to further optimize the impeller power consumption by changing the impeller diameter, type, and blade thickness, as discussed in the previous section.

Simple Model. A number of experiments were conducted in this study to evaluate the effects of different parameters on (C_v)_{osc}. It is of interest here to develop a simple mathematical model to predict (C_v)_{osc} for different operating conditions.

The presence of solids can be expected to influence the impeller performance by modifying the suspension viscosity, local density, and vortex structure in the vicinity of impeller

blades.⁹ At higher loadings, the effect of solid particles on the impeller hydrodynamics becomes more significant and, thus, influences the power consumption. Taking this into account, the following empirical correlation between power consumption and C_v was proposed by Bubbico et al.⁸

$$P = N_p(1 + kC_v)\rho_w N^3 D^5 \quad (9)$$

where P (W) is the power required to satisfy the just-off-bottom condition, ρ_w (kg/m^3) is the density of water, $N_p(1 + kC_v)$ is defined as the actual impeller power number, C_v represents the volumetric solids concentration, and the parameter k is regarded as a measure of the additional energy dissipation due to the presence of solid particles. The mass of solids in the agitated vessel can be expressed as

$$M_s = \rho_s V_s = \rho_s V C_v \quad (10)$$

where M_s is the mass of solids, ρ_s represents the solid density, V_s represents the volume of solids, and V represents the total volume of the liquid–solid system. Combining eqs 9 and 10, we get

$$\varepsilon_{js} = \frac{P}{M_s} = \left(N_p \frac{\rho_w}{V \rho_s} N^3 D^5 \right) \left(\frac{1}{C_v} + k \right) \quad (11)$$

According to ref 5, the correlation between N_{js} and X can be represented as

$$N_{js} = S \frac{\nu^{0.1} d^{0.2} (g \Delta \rho / \rho_l)^{0.45} X^a}{D^{0.85}} \propto X^a \quad (12)$$

where N_{js} is the impeller speed (rps), ρ_l is the liquid density (kg/m^3), $\Delta \rho$ is the difference in densities of solid and liquid (kg/m^3), d is the solid mean particle diameter (m), D is the impeller diameter (m), S is a dimensional coefficient based on impeller type, ν is the kinematic viscosity ($\text{m}^2 \text{s}^{-1}$), and X is the solids loading ratio (weight of solids $\times 100$ /weight of liquid).

However, X is a function of C_v as follows

$$X = \left(\frac{\rho_s}{\rho_w} \right) \left(\frac{C_v}{1 - C_v} \right) \times 100 \quad (13)$$

Combining eqs 11–13, we obtained the following equation to determine the specific power dissipated by each impeller at N_{js}

$$\begin{aligned} \varepsilon_{js} &= \frac{P}{M_s} = \nu^{0.3} \left(\frac{100 C_v}{1 - C_v} \frac{\rho_s}{\rho_w} \right)^{3a} \left(\frac{1}{C_v} + k \right) \\ &\quad \left(\frac{S d^{0.2} (g \Delta \rho / \rho_l)^{0.45}}{D^{0.85}} \right)^3 \left(\frac{N_p \rho_w D^5}{V \rho_s} \right) \end{aligned} \quad (14)$$

Based on Thomas's correlation,^{17,18} the kinematic viscosity of the slurry can be estimated as a function of solids concentration using the equation

$$\begin{aligned} \nu &= \frac{\eta_{\text{slurry}}}{\rho_{\text{slurry}}} \\ &= \frac{\eta_r [1 + 2.5C_v + 10.05C_v^2 + 0.0273 \exp(16.6C_v)]}{\rho_s C_v + \rho_w (1 - C_v)} \end{aligned} \quad (15)$$

where η_r is the viscosity of the liquid phase. Thus, we have

$$\varepsilon_{js} = G \left(\frac{100 C_v \rho_s}{(1 - C_v) \rho_w} \right)^{3a} \left(\frac{1}{C_v} + k \right) \nu^{0.3} \quad (16)$$

where G is the product of the last two groups (in parentheses) in eq 14, which is a constant for a given solid–liquid system and tank and impeller geometries. Based on eq 16, ε_{js} can be regarded as a function of C_v only for any given geometry due to the fact that the parameter k is associated with the impeller type and particle size. This equation also indicates that ε_{js} is a measure of the additional energy dissipation due to the presence of the solid phase.

The exponent a for low to medium C_v values (0.09–0.20 v/v) is approximately equal to 0.13 according to Zweitering.⁵ It is assumed that $a \approx 0.13$ here from low to high C_v , although it was found that a is higher than 0.13 for very high C_v values (0.4–0.52 v/v).¹¹

The ε_{js} values predicted using eq 16 as a function of C_v are shown in Figure 17 for different impellers. For the sake of

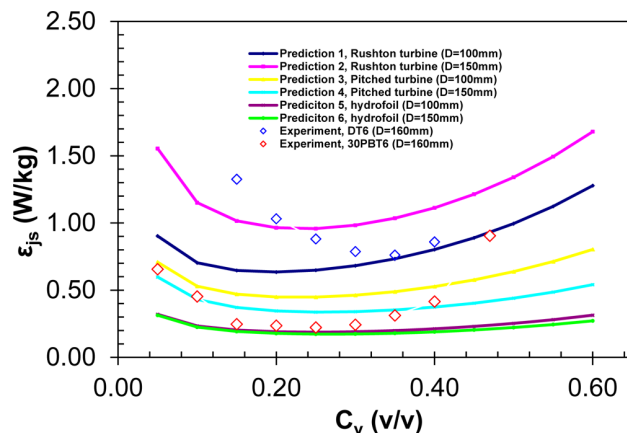


Figure 17. ε_{js} predicted using eq 16 vs C_v for $a = 0.13$, $\rho_w = 1000 \text{ kg}/\text{m}^3$, and $\rho_s = 2500 \text{ kg}/\text{m}^3$. Refer to Table 5 for values of power number N_p and k ; $S = 2$.

comparison, experimental values of ε_{js} for impellers DT6 and 30PBT6 are also shown in Figure 17. The trends in predicted ε_{js} values confirm the presence of $(C_v)_{osc}$ at which ε_{js} is the minimum, regardless of the impeller type used. However, the predicted ε_{js} values exhibit a flat trend at higher C_v (0.40–0.60 v/v), indicating that they are not valid in that range. This finding suggests that Zweitering's correlation has limitations and is not valid at high C_v (>0.4 v/v). The predicted ε_{js} values show that $(C_v)_{osc}$ is in the range of 0.20–0.25 v/v for the three impeller types used in this work (Table 5). It is clear that ε_{js} is a function of S , but the value of $(C_v)_{osc}$ is not affected by S , as can be seen from eq 12.

From the results shown above, although we cannot perfectly predict the ε_{js} values due to the assumptions made above, it can still be said that the model eq 16 predicted $(C_v)_{osc}$ satisfactorily. However, the flow pattern in the suspension was assumed to be turbulent in developing this equation even at high C_v because eq 9 was used in estimating Re . Further improvements in the equation can be made by considering the changes in the flow pattern as C_v increases.

Particle Dispersion at N_{js} . A typical solids concentration profile measured by Hicks et al.¹⁵ at N_{js} is shown in Figure 18. The system consisted of a Chemineer HE-3 impeller and glass beads with a mean diameter of 200 μm and a density of 2500

Table 5. Optimum Solids Concentration: Results Predicted Based on Eq 16 with Baffles Installed

prediction	D (mm)	N_p	k	$(C_v)_{osc}$	
				predicted ^a	experimental
Rushton Turbine					
1	100	3.338	2.794	0.20	0.35
2	150	3.502	2.447	0.25	0.35
Pitched Turbine					
3	100	1.582	2.227	0.25	0.25–0.30
4	150	1.391	1.315	0.25	0.25–0.30
Hydrofoil					
5	100	0.735	1.603	0.25	0.30
6	150	0.734	1.169	0.25	0.30

^aBased on Figure 17.

kg/m³. The axial solids concentration profile shown in the graph indicates that the solids concentration is relatively constant throughout much of the slurry but falls rapidly to zero at around the cloud height, H_s . Hicks et al.¹⁵ pointed out that similar behavior can be found at other operating conditions and suggested that “although the cloud height does not give the most detailed information possible, it does provide a sound qualitative basis for design”. They believed that dispersion of particles can be quantified by the normalized slurry cloud height (H_s/H), where H_s represents the slurry cloud height (m) and H is the liquid height (m). Based on the above discussion, the following criteria should be met to maintain a homogeneous condition in solid–liquid mixing, which is desirable in many industrial applications such as catalytic reactors and slurry holding tanks

$$H_s = H$$

$$H_B = 0$$

Experimental values of normalized bed heights (H_s/H) at N_{js} for impellers DT6, 30PBT6, and A310 are shown for selected C_v values in panels a–c, respectively, of Figure 19. Of these three impellers, DT6 has the best performance in dispersing the particles at N_{js} , as it can lead to nearly complete dispersion of particles ($H_s/H = 1$) from low to high C_v (0.15–0.40 v/v), regardless of the baffle arrangement. Figure 19b,c suggests that the removal of baffles plays an important role in improving the particle dispersion for impellers 30PBT6 and A310, as higher

H_s/H values are obtained under unbaffled conditions. It can also be seen in Figure 19b that it is not possible to fully disperse the particles throughout the tank at N_{js} with impeller 30PBT6, regardless of the C_v value used. In contrast, full dispersion of particles is achieved with impeller A310 under unbaffled conditions although at relatively lower C_v values of 0.25 and 0.30 v/v (Figure 19c). These results led us to conclude that the removal of baffles helps not only in improving the off-bottom suspension of solids but also in dispersing the solids better.

Optimized Tank Design. A case example is shown in Figure 20 to illustrate the benefits of adopting some of the optimization methods highlighted in the earlier sections of this article.

Figure 20a shows a premodified design in which the solid–liquid mixing tank was equipped with an A310 impeller, a widely used axial-flow impeller for solids suspension. To the authors’ best knowledge, operating solid–liquid mixing tanks with relatively low solids concentrations ($C_v < 0.20$ v/v) is still common practice in mineral industries. Based on this fact, a low solids concentration ($C_v = 0.10$ v/v) was chosen for this example. The premodified design (Figure 20a) had four baffles, as baffled tanks are generally considered to be “standard” in solid–liquid mixing and a considerable effort has been made in studying impeller power requirements for solids suspensions in baffled tanks.^{1,6–8,11} Poor utilization of tank volume can be seen clearly in the premodified system from a relatively low value for H_s/H (= 0.68). Values of other important operating parameters are shown in Figure 20a.

Details of a new (modified) design are shown in Figure 20b. The tank had a DT6 impeller and no baffles. The tank was operated at a higher solids concentration ($C_v = 0.33$ v/v), but it required relatively lower N_{js} (169 rpm). It can be noted that the degree of particle dispersion improved significantly, as indicated by a larger H_s/H value (~1) obtained in this case. From this observation, it is quite evident that greater energy efficiency in this case was achieved by operating the tank at higher C_v but using a lower $\epsilon_{js} = 0.13$ W/kg simply by changing the impeller type and removing the baffles. In other words, a substantial increase in C_v (3.3 times) has been achieved with an 18% reduction in ϵ_{js} with minimal design changes. In comparison, the premodified design required a much higher ϵ_{js} (= 0.37 W/kg) for suspending lower $C_v = 0.10$ v/v. The changes mentioned above helped in minimizing the capital costs,

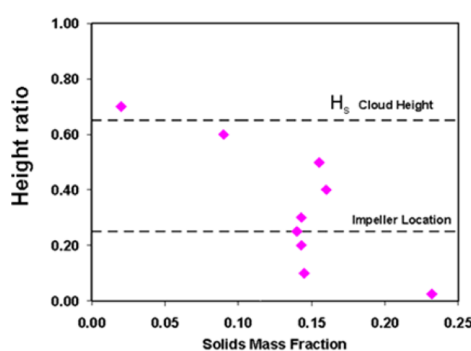


Figure 18. Typical axial solids concentration profile.¹⁵ Impeller: HE-3. Conditions: $d_p = 200 \mu\text{m}$, $D/T = 0.35$, $C/T = 0.25$, $H/T = 1$, solids mass fraction = 0.116.

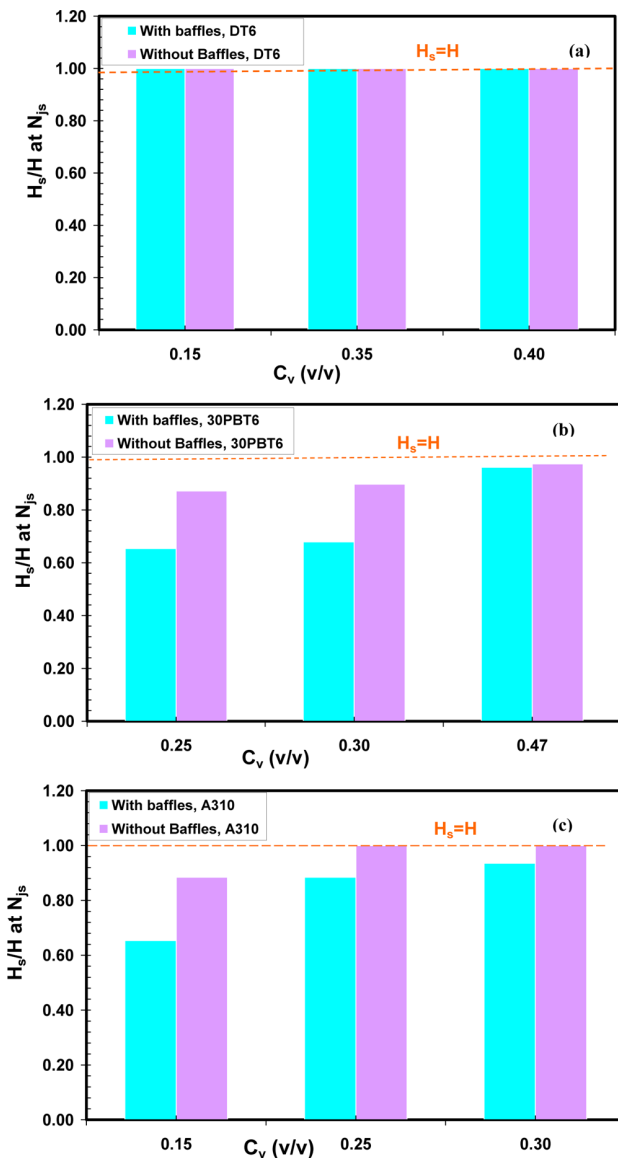


Figure 19. Ratio of cloud and liquid heights (H_s/H) at N_{js} vs C_v when baffled and unbaffled: (a) radial-flow impeller, DT6; (b) mixed-flow impeller, 30PBT6; (c) axial-flow impeller, A310. $d_{50} = 90 \mu\text{m}$.

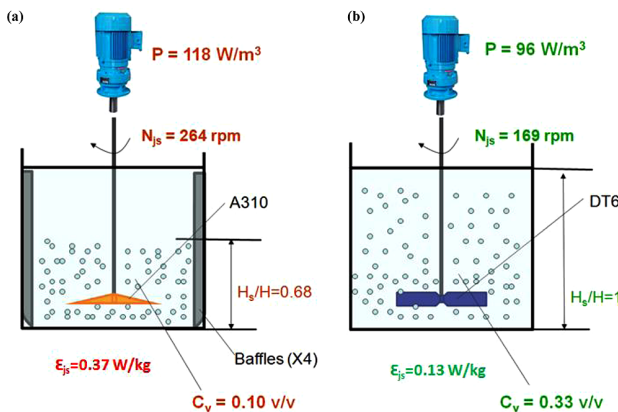


Figure 20. Design modification for an agitated reactor: (a) existing design, $C_v = 0.10 \text{ v/v}$; (b) modified design, $C_v = 0.33 \text{ v/v}$. $d_{50} = 90 \mu\text{m}$.

which otherwise would have included the cost of retrofitting the gear box for a speed upgrade.

The overall benefits of process intensification of solid–liquid mixing tanks that include changing the tank design and operating the tank with an increased solids concentration can be thus summarized as follows: (a) maintaining (or even reducing) impeller power consumption and agitator speed, (b) increasing yield or throughput, (c) improving energy efficiency, and (d) improving particle dispersion.

CONCLUSIONS

The specific impeller power required for the off-bottom suspension of solids was studied over a range of solids concentrations and particle sizes. It established that the specific impeller power at N_{js} expressed on the basis of total volume of suspension (P_{js}/V) increases rapidly with increasing solids concentration for $C_v > 0.30 \text{ v/v}$. Nevertheless, when the specific power input is considered in terms of the mass of solids suspended ($\epsilon_{js} = P_{js}/M_s$), it decreases with solids concentration up to a critical value and increases beyond that. This result is observed for radial (DT6), mixed (30PBT6), and axial (A310) flow impellers used in this work under baffled and unbaffled conditions.

It is also found that ϵ_{js} can be minimized by operating the vessel at a suitable solids concentration in the range of 0.20–0.35 v/v for the impeller types and baffle conditions used in this study. Under baffled conditions, the optimum solids concentration [$(C_v)_{osc}$] is influenced by the impeller type and impeller dimensions. Under unbaffled conditions, however, $(C_v)_{osc}$ is independent of particle size but is influenced by impeller type.

Higher-power-number radial-flow impellers are found to be more energy efficient than lower-power-number axial-flow impellers for suspending fine particles under unbaffled conditions. It appears that the effect of removing baffles is more significant at lower C_v for the radial-flow impeller (DT6) because it leads to a significant reduction in ϵ_{js} . At higher C_v , there is also a reduction in ϵ_{js} for impeller DT6 because of the removal of baffles, but the extent of the reduction is not as significant as that at the low solids concentration. Of all the impellers used, the radial-flow impeller (DT6) is the most sensitive to the removal of baffles irrespective of C_v . These results imply that DT6 is the most energy efficient under unbaffled conditions compared to the axial- and mixed-flow impellers tested.

A simple mathematical model based on Zweitering's correlation for N_{js} is found to predict the optimum solids concentration satisfactorily. It is suggested that the removal of baffles helps not only in improving the off-bottom suspension of solids but also in dispersing them more effectively.

AUTHOR INFORMATION

Corresponding Authors

*E-mail: rchrp@rmit.edu.au.

*E-mail: steven.wang@csiro.au.

Notes

The authors declare no competing financial interest.

ACKNOWLEDGMENTS

The research was supported financially by Fluids Engineering Group, CSIRO, Australia.

NOMENCLATURE

- B = baffle width (m)
 C_v = solids volume concentration (v/v)
 $(C_v)_{\max}$ = maximum solids volume concentration (v/v)
 $(C_v)_{\text{osc}}$ = optimum solids concentration (v/v)
 d = particle size (mm)
 D = impeller diameter (m)
 H = liquid level (m)
 H_B = settled bed height (m)
 H_S = slurry cloud height (m)
 k = impeller constant in eq 9
 M_s = mass of solids (kg)
 N = impeller speed (rev/s, rpm)
 N_{js} = impeller speed for just-off-bottom solids suspension (rpm)
 N_p = power number
 P = power (W)
 P_{js} = agitator power for achieving just-off-bottom solids suspension (W)
 S = dimensional coefficient in eq 12
 t = blade thickness (m)
 T = tank diameter (m)
 V = tank volume (m^3)
 W = blade width (m)
 X = solid loading ratio (kg/kg)
 ϵ_{js} = specific power input, agitator power per unit solids mass at the just-off-bottom solids suspension condition (P_{js}/M_s) (W/kg)
 ϵ_{js}^{-1} = mass of solids suspended per Watt at the just-off-bottom solids suspension condition (M_s/P_{js}) (kg/W); power efficiency factor.
 $(\epsilon_{js})_{\min}$ = specific power consumption at $(C_v)_{\text{osc}}$ (W/kg)
 η_r = carrier fluid viscosity (Pa·s)
 η_{slurry} = slurry viscosity (Pa·s)
 ρ_l = liquid density (kg/m^3)
 ρ_s = solids density (kg/m^3)
 ρ_{slurry} = slurry density (kg/m^3)

REFERENCES

- (1) Nienow, A. W. Suspension of Solid Particles in Turbine Agitated Baffled Vessels. *Chem. Eng. Sci.* **1968**, *23*, 1453–1459.
- (2) Chapman, C. M.; Nienow, A. W.; Cooke, M.; Middleton, J. C. Particle–Gas–Liquid Mixing in Stirred Vessels. Part II: Gas–Liquid Mixing. *Chem. Eng. Res. Des.* **1983**, *61*, 82–95.
- (3) Chapman, C. M.; Nienow, A. W.; Cooke, M.; Middleton, J. C. Particle–Gas–Liquid Mixing in Stirred Vessels. Part III: Three Phase Mixing. *Chem. Eng. Res. Des.* **1983**, *61*, 167–181.
- (4) Nienow, A. W. The Suspension of Solid Particles. In *Mixing in the Process Industries*. 2nd ed.; Harnby, N., Edwards, M. F., Nienow, A. W., Eds.; Butterworths: London, 1992; Chapter 16, pp 364–393.
- (5) Zwietering, T. N. Suspending of Solid Particles in Liquid by Agitators. *Chem. Eng. Sci.* **1958**, *8*, 244–253.
- (6) Raghava Rao, K. S. M. S.; Rewatkar, V. B.; Joshi, J. B. Critical Impeller Speed for Solid Suspension in Mechanically Agitated Contactors. *AIChE J.* **1998**, *34*, 1332–1340.
- (7) Dreher, G. R.; Ahmed, N.; Jameson, G. J. Suspension of High Concentration Solids in Mechanically Stirred Vessels. *Inst. Chem. Eng. Symp. Ser.* **1994**, *136*, 41–48.
- (8) Bubbico, R.; Di Cave, S.; Mazzarotta, B. Agitation Power for Solid–Liquid Suspensions Containing Large Particles. *Can. J. Chem. Eng.* **1998**, *76*, 428–432.
- (9) Kasat, G. R.; Pandit, A. Review on Mixing Characteristics in Solid–Liquid and Solid–Liquid–Gas Reactor Vessel. *Can. J. Chem. Eng.* **2005**, *83*, 618–643.
- (10) Wu, J.; Nguyen, B.; Graham, L. Energy Efficient High Solids Loading Agitation for the Mineral Industry. *Can. J. Chem. Eng.* **2010**, *88*, 287–294.
- (11) Wu, J.; Zhu, Y. G.; Pullum, L. Suspension of High Concentration Slurry. *AIChE J.* **2002**, *48*, 1349–1352.
- (12) Dreher, G. R.; Ahmed, N.; Jameson, G. J. An Optimum Concentration for the Suspension of Solids in Stirred Vessels. In *Mixing and Crystallization*; Sen Gupta, B., Ibrahim, S., Eds.; Kluwer Academic Publishers: Dordrecht, The Netherlands, 2000; pp 83–94.
- (13) Wu, J.; Nguyen, B.; Graham, L. Mixing Intensification for the Mineral Industry. *Can. J. Chem. Eng.* **2010**, *88*, 447–454.
- (14) Bujalski, W.; Takenaka, K.; Paolilni, S.; Jahoda, M.; Paglanti, A.; Takahashi, A.; Nienow, A. W.; Etchells, A. W. Suspensions and Liquid Homogenisation in High Solids Concentration Stirred Chemical Reactors. *Trans. Inst. Chem. Eng.* **1999**, *77*, 241–247.
- (15) Hicks, M. T.; Myers, K. J.; Bakker, A. Cloud Height in Solids Suspension Agitation. *Chem. Eng. Commun.* **1997**, *160*, 137–155.
- (16) Wang, S.; Boger, D.; Wu, J. Energy Efficient Solids Suspension in an Agitated Vessel–Water Slurry. *Chem. Eng. Sci.* **2012**, *74*, 233–243.
- (17) Honek, T.; Hausnerova, B.; Saha, P. Relative Viscosity Models and Their Application to Capillary Flow Data of Highly Filled Hard-Metal Carbide Powder Compounds. *Polym. Compos.* **2005**, *26*, 29–36.
- (18) Thomas, D. G. Transport Characteristics of Suspension: VIII. A Note on the Viscosity of Newtonian Suspensions of Uniform Spherical Particles. *J. Colloid Sci.* **1965**, *20*, 267–277.
- (19) Fedors, R. F. Variability of Ultimate Properties of Elastomers. *J. Appl. Polym. Sci.* **1975**, *19*, 787–790.
- (20) Geisler, R. K.; Buurman, C.; Mersmann, A. B. Concept for Scale-up of Solids Suspension in Stirred Tanks. In *Proceedings: 7th European Conference on Mixing*; Koninklijke Vlaamse Ingenieursvereniging: Brugge, Belgium, 1991; pp 451–459.
- (21) Armenante, P. M.; Li, T. Minimum Agitation Speed for Off-Bottom Suspension of Solids in Agitated Vessels Provided with Multiple Flat-Blade Impellers. *AIChE Symp. Ser.* **1993**, *89*, 105–111.
- (22) Nocentini, M. F.; Magell, F.; Pasquali, G. On the Modeling of the Gas Behaviour of Gas–Liquid Vessels Stirred with Multiple Impellers. In *Mixing: Proceedings of the 6th European Conference, Pavia, Italy, 24–26 May 1988*; Associazione Italiana di Ingegneria Chimica (AIDIC): Milan, Italy, 1988; p 337.
- (23) Dutta, N. N.; Pangarkar, V. G. Critical Impeller Speed for Solid Suspension in Multi-Impeller Agitated Contactors: Solid–Liquid System. *Chem. Eng. Commun.* **1995**, *137*, 135–146.